Hindawi
Geofluids
Volume 2021, Article ID 6838092, 12 pages
https://doi.org/10.1155/2021/6838092

Research Article

Experimental Study of the Influence of Moisture Content on the Mechanical Properties and Energy Storage Characteristics of Coal

Nan Liu,[1,2] **Chuanming Li**,[1,2] **Ruimin Feng**,[3] **Xin Xia**,[1,2] **and Xiang Gao**[1,2]

[1]*School of Mining Engineering, Anhui University of Science and Technology, Huainan 232001, China*
[2]*Key Laboratory of Coal Mine Safety and Efficiently Caving of Ministry of Education, Anhui University of Science and Technology, Huainan 232001, China*
[3]*Department of Civil Engineering, University of Arkansas, 4190 Bell Engineering Center, Fayetteville, AR 72701, USA*

Correspondence should be addressed to Chuanming Li; chuanmingli@126.com

Received 31 May 2021; Accepted 1 July 2021; Published 24 July 2021

Academic Editor: Zhijie Wen

Rock burst occurs frequently as coal mining depth goes deeper, which seriously impacts the safety production of underground coal mines. Coal seam water injection is a technique commonly used to prevent and control such accidents. Moisture content is a critical factor tightly related to rock burst; however, an in-depth insight is required to discover their relationship. In this study, the influence of moisture content on the mechanical properties of coal and rock burst tendency is explored via multiple measurement techniques: uniaxial compression test, cyclic loading/unloading test, and acoustic emission (AE) test. These tests were performed on coal samples using the MTS-816 rock mechanics servo testing machine and AE system. The testing results showed that with the increase in moisture content, the peak strength and elastic modulus of each coal sample are reduced while the peak strain increases. The duration of the elastic deformation phase in the complete stress-strain curves of coal samples is shortened. As the moisture content increases, the area of hysteretic loop and elastic energy index W_{ET} of each coal sample are reduced, and the impact energy index K_E is negatively correlated with the moisture content, whereas dynamic failure time is positively correlated with the moisture content, but this variation trend is gradually mitigated with the continuous increase of moisture content. The failure of the coal sample is accompanied by the sharp increase in the AE ring-down count, whose peak value lags behind the peak stress, and the ring-down count is still generated after the coal sample reached the peak stress. With the increase in moisture content, the failure mode of the coal sample is gradually inclined to tensile failure. The above test results manifested that the strength of the coal sample is weakened to some extent after holding moisture, the accumulative elastic energy is reduced in case of coal failure, and thus, coal and rock burst tendency can be alleviated. The study results can provide a theoretical reference for studying the fracture instability of moisture-bearing coal and prevention of coal and rock burst by the water injection technique.

1. Introduction

As underground coal mining gradually goes deeper, rock burst has become a dynamic disaster seriously threatening the coal mine safety production [1–3]. As an important index used to measure the possibility of rock burst occurrence, the burst tendency of coal is affected by various factors, among which moisture content is a highly significant influencing factor [4]. Coal seam water injection is a common technique for preventing and controlling rock burst [5]. Therefore, studying the influence laws of moisture content on the mechanical properties of coal and its burst tendency will be of great theoretical and practical significance.

Many researchers have studied the influence of moisture content on the mechanical properties of coal body, mainly concentrating on the compressive strength [6–10], the tensile strength [10–14], and the physical properties under triaxial tests [15–18]. Based on a widely accepted viewpoint, a piece of coal, if containing water, will go through creep damage, which also damages coal strength [19, 20]. Auxiliary monitoring means are generally adopted by many scholars to indirectly reflect the strength loss relation of coal [21, 22].

Acoustic emission (AE), a mature technique to monitor sample failure process, can reflect the precursor information of compression-induced fracture instability of coal on the basis of the AE signal [23], and the peak value of AE ring-down count appears nearby the peak stress, making it applicable to geotechnical engineering, such as coal mining, slope, tunnel, and bridge [24, 25]. AE signal has a favorable corresponding relationship with the complete stress-strain curve of coal [26–29]. The increase in the moisture content of coal will repress the occurrence of AE events [30–32], and meanwhile, the load-carrying induced failure of moisture-containing coal-rock mass is usually accompanied by the changes in its internal structure and physicochemical properties, as well as the energy released in forms of AE, recovery of elastic energy, and so on [33, 34].

Most of the abovementioned studies have been focused on the influence laws of moisture content in coal on its mechanical properties, which has, to a great extent, deepened the understanding of fracture instability characteristics of moisture-containing coal samples, but the influence of high moisture content on the mechanical properties and burst tendency of coal has been rarely involved. Therefore, studying the influence of high moisture content on the mechanical properties and burst tendency of coal under waterlogging effect will be of great pertinence and significant research value.

Figure 1: Ready condition of the coal sample.

Figure 2: Some coal samples after processing.

2. Introduction of Test

2.1. Testing Equipment and Sample Preparation. The testing system used in this study was mainly composed of two setups. The MTS-816 rock mechanics servo testing machine was used for the uniaxial compression and cyclic loading/unloading, and the DS5 AE system was employed to monitor the AE data in the load-carrying process of coal samples. The AE system was equipped with a probe to acquire signals, which was bonded onto the surface of the coal pillar using a coupling agent and mighty adhesive tape. Based on the past testing experience, the sampling frequency of the amplifier was set to 40 dB, with a threshold value of 50 dB. The MTS-816 rock mechanics servo testing machine consisted of a loading/unloading subsystem and automatic data acquisition subsystem, which can be conveniently operated via the computer. Meanwhile, the testing process can be manually intervened, and the control mode, test parameters, and test procedures can also be altered. Figure 1 pictorially shows the ready condition of the coal sample.

To reduce the measurement errors induced by sample preparation, a few coal samples were collected from the same place and taken to the laboratory, followed by the coring, cutting, and grinding procedures. Ultimately, they were processed into cylindrical samples with a diameter of 50 mm and a height of 100 mm. The coal samples were numbered as a1-a9 and b1-b9, where a1-a9 were used to perform the mechanical property test and AE test under uniaxial compression, and b1-b9 were used to test the energy evolution characteristics under cyclic loading. The pictures of the well-prepared coal samples are shown in Figure 2.

2.2. Testing Program and Process. Before the test was started, all coal samples were soaked in water to study their water absorption laws. Firstly, the mass of each sample was weighed and calculated, it was then soaked in water until reaching the prescribed mass, and meanwhile, the time needed by the sample to reach the prescribed moisture content was recorded. Lastly, it was maintained in a closed container for 24 h, and the test was finally commenced. The moisture content ω is calculated by Formula (1), and the results are listed in Table 1.

$$\omega = \frac{M_1 - M_2}{M_2} * 100\%. \quad (1)$$

The uniaxial compression test and cyclic loading/unloading tests were carried out in accordance with the standard of the China National Coal Association (GB/T 25217.2-2010). In the uniaxial compression test, the stress loading was applied using MTS-816 on each coal sample at a rate of 0.5 MPa/s. In the cyclic loading/unloading test, the load was applied to each sample at a rate of 0.5 MPa/s until reaching 75%–85% of average uniaxial strength, and then, it was unloaded to 5% of uniaxial strength at the same rate, and thereafter, the coal sample was cyclically loaded and unloaded in this way. The maximum strength

Table 1: Mechanical parameters of some coal samples.

Preloading condition	No.	Moisture content	Preloading condition	No.	Moisture content
Uniaxial compression test	a1	16%	Loading/unloading test	b1	16%
	a2	17%		b2	17%
	a3	17%		b3	18%
	a4	18%		b4	18%
	a5	19%		b5	19%
	a6	20%		b6	21%
	a7	21%		b7	22%
	a8	22%		b8	23%
	a9	25%		b9	25%

value of cyclic loading each time was 5% greater than the maximum strength value at the previous loading stage until the coal failure. During the testing process, the MTS-816 was synchronously operated with the AE system, where the MTS-816 system automatically acquired data, recorded the stress, strain, and time, and drew the stress-strain curves, and the AE system realized the automatic acquisition of the event number.

3. Analysis of Test Results

3.1. Effects on Mechanical Properties of Coal Samples. The complete stress-strain curves of several coal samples are shown in Figure 3. Each curve can be divided into five phases: fracture compaction, elastic, yield, failure, and postpeak phases. Once the loading got started, the complete stress-strain curve was obviously bent, and as the moisture content increased, the slope of the curve was obviously reduced, namely, the duration of the elastic deformation phase was shortened and that of the plastic zone in the postpeak phase was lengthened, and the overall curve was inclined to rightward offset, that is, the possibility of plastic failure was increased. The moisture state significantly led to the mechanical damage of coal samples.

The influences of different moisture contents on the peak strength and peak strain of coal samples are shown in Figure 4. Peak strain, referring to the strain of the coal sample in case of peak stress, denotes the deformation degree of the coal sample when experiencing a failure. As shown in the figure, the peak strength of the coal sample has a negative linear correlation with the moisture content, and the peak strain shows a positive linear correlation with the moisture content. As the moisture content increases from 16% to 25%, the compressive strength declines from 4.28 MPa to 1.71 MPa, with the decreasing amplitude approaching 60%. When the peak strain increases from 0.01168 to 0.01736, the increasing amplitude is approximately 32%. Therefore, the coal samples with high moisture content showed more obvious plastic failure characteristics. A possible reason is that after containing water molecules, the enhanced plastic ability of coal particles lengthens the fracture compaction phase and weakens the friction coefficient and cohesion between internal coal particles [35],

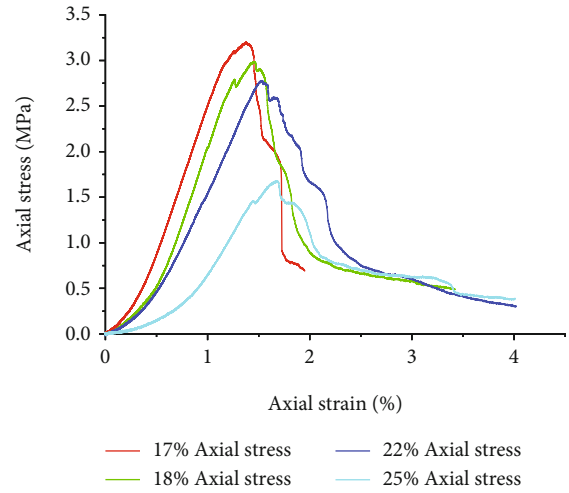

Figure 3: Complete stress-strain curves of coal samples with different moisture contents.

further indicating that the higher moisture content leads to the lower peak strength, the higher peak strain, and the more obvious coal "softening."

Elastic modulus reflects the coal-rock deformation resistance in the elastic deformation phase. Based on the linear relationship between stress and strain in the elastic deformation phase, the elastic modulus of coal and rock [36] can be calculated by

$$E = \frac{\sigma_2 - \sigma_1}{\mu_2 - \mu_1}, \tag{2}$$

where σ is the stress at one point on the complete stress-strain curve, MPa; μ is the corresponding strain of the complete stress-strain curve.

Figure 5 and Table 2 show that the elastic modulus of coal presents a declining trend with the increase in moisture content, showing an overall negative correlation. The elastic moduli of most samples are roughly 0.35 GPa, possibly because the high moisture content in the coal sample leads to an internal crack closure and tremendous friction

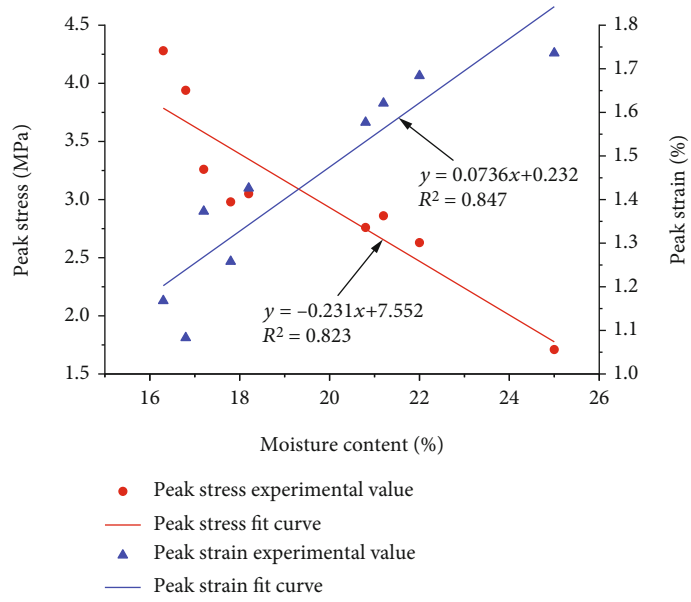

Figure 4: Influence curves of peak stress and peak strain of coal samples with different moisture contents.

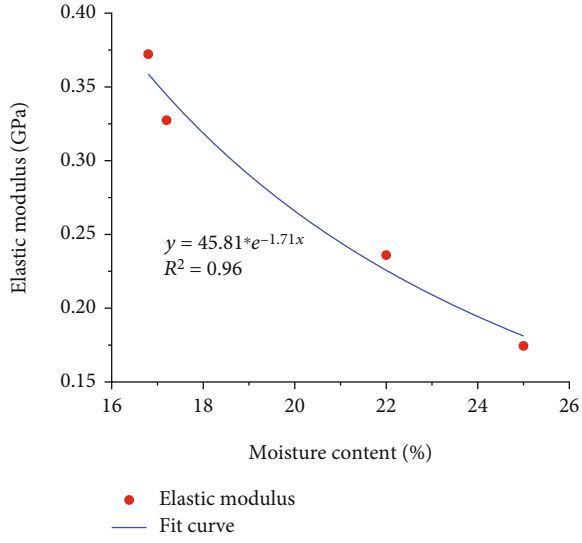

Figure 5: Influence curve of moisture content on elastic modulus of the coal sample.

coefficient, which makes it difficult for the fracture surface to slide during failure [37].

Under hydraulic pressure, the elastic modulus of the coal sample will also be reduced, and the relation is as follows [38]:

$$E = c - dp, \tag{3}$$

where c and d are coefficients and p is the hydrostatic pressure.

From Formula (3) and Figure 5, it can be known that elastic modulus will decline more obviously under high hydraulic pressure. Therefore, coal is prone to deformation and even failure under high moisture content and high hydraulic pressure.

3.2. Energy Evolution Characteristics of Coal Samples. The primary cause for a dynamic disaster is energy release [39]. Rock loading/unloading is a process of energy accumulation, dissipation, and release, and the annular region enclosed by the loading curve segment of the coal sample and the unloading curve segment formed in the previous cycle is a hysteretic loop [40, 41].

Based on the energy conservation law and thermodynamics, the mechanical energy of the MTS-816 rock mechanics servo testing machine can be largely divided into two parts: internal elastic strain energy temporarily stored and plastic strain energy. The relationship between those two can be expressed by Formula (4) as follows:

$$U = U_1 + U_2 = \sum_{i=1}^{n} \frac{1}{2}(\sigma_{i+1} + \sigma_i) \times (\varepsilon_{i+1} - \varepsilon_i), \tag{4}$$

$$\begin{aligned} U_1 &= \int_a^b \sigma d\varepsilon, \\ U_2 &= \int_b^c \sigma d\varepsilon, \end{aligned} \tag{5}$$

where U is the total energy generated by the work done by the external load to the rock sample, being the area under the ith loading curve; U_1 is the plastic strain energy, being the area of the hysteretic loop in the ith cycle; and U_2 is the elastic strain energy, being the area under the ith unloading curve. σ_i and ε_i are the corresponding stress and strain values at each point on the stress-strain curve.

Table 2: Mechanical parameters of some coal samples.

Loading condition	No.	Moisture content	Loading rate	Elasticity modulus (GPa)	Peak strength (MPa)
Uniaxial compression failure	a2	17%	0.5 MPa/s	0.3722	3.94
	a4	18%		0.3274	3.05
	a8	22%		0.2361	2.63
	a9	25%		0.1744	1.71

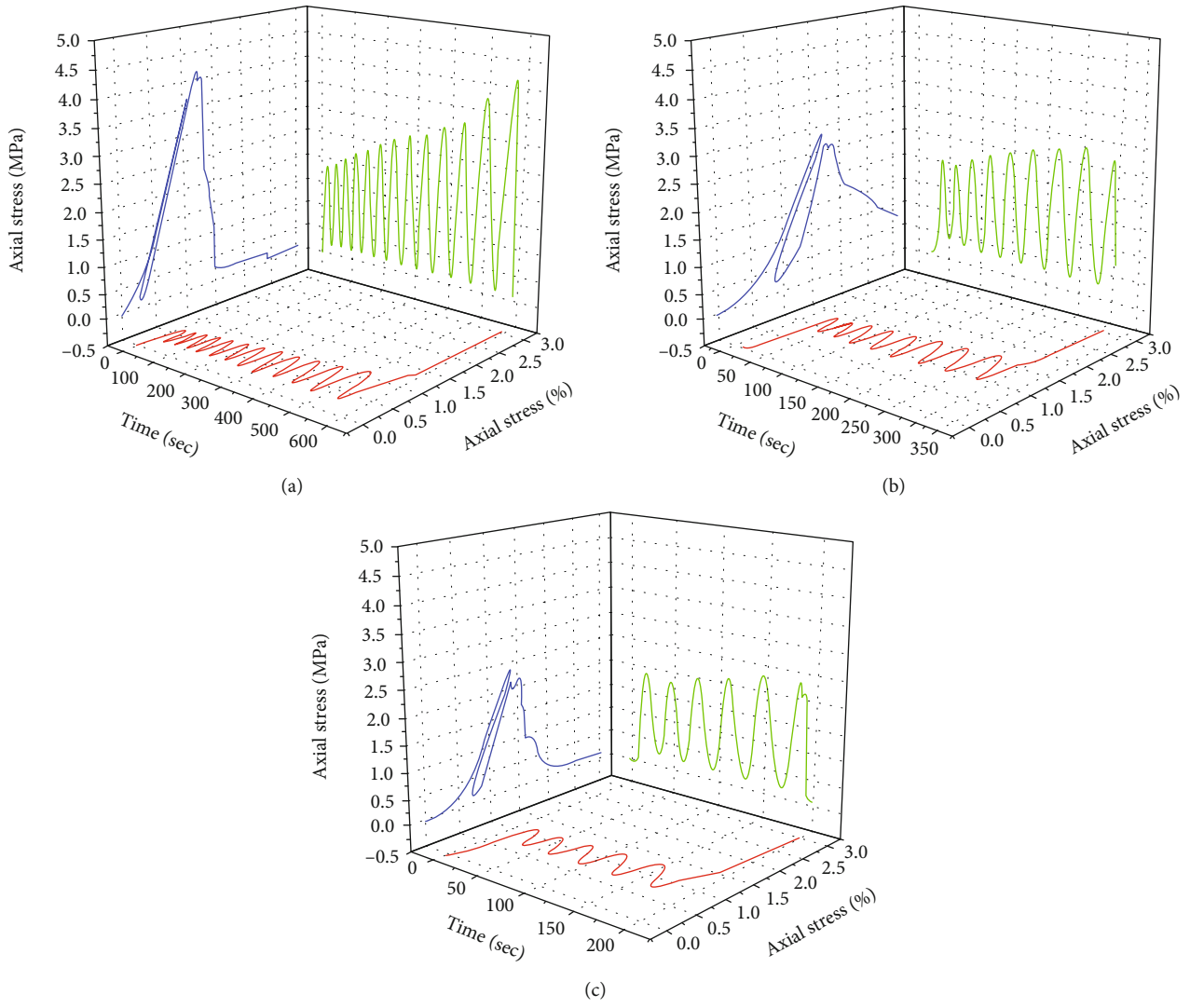

Figure 6: Cyclic loading/unloading curves of coal samples with different moisture contents ((a) 18%; (b) 21%; (c) 25%).

Table 3: Calculation results of cyclic loading energy of coal samples.

Loading mode	No.	Moisture content	Number of cyclic stages before failure	Total strain energy U	Area of hysteretic loop U_1 /J·m^{-3}	Recoverable strain energy U_2
Cyclic loading/unloading	b3	18%	12	2.95441	0.39274	2.56167
	b6	21%	8	2.42494	0.44268	1.98226
	b9	25%	5	2.00783	0.54268	1.46515

Table 4: Classification of burst tendency of coal.

	Type Burst tendency	Type I No	Type II Weak	Type III Strong
Index	Dynamic failure time/ms	$D_T > 500$	$50 < D_T \leq 500$	$D_T \leq 50$
	Elastic energy index	$W_{ET} < 2$	$2 \leq W_{ET} < 5$	$W_{ET} \geq 5$
	Impact energy index	$K_E < 1.5$	$1.5 \leq K_E < 5$	$K_E \geq 5$
	Uniaxial compressive strength (MPa)	$R_C < 7$	$7 \leq R_C < 14$	$R_C \geq 14$

The cyclic loading/unloading images of the coal samples with moisture contents of 18%, 21%, and 25% were selected as an example demonstration. As shown in Figure 6 and Table 3, the unloading curve of the coal sample was slightly lower than the loading curve, and the total strain energy presents a declining trend. For each coal sample in this test, the area of the hysteretic loop was gradually enlarged with the increase in moisture content, indicating that the dissipated energy gradually increases. The peak stresses failing three coal samples are 3.112 MPa, 2.663 MPa, and 2.315 MPa, after the 13-stage, 9-stage, and 6-stage cyclic loading, respectively. The peak stress leading to the failure of the coal sample under the cyclic loading/unloading is not much different from the peak stress of the coal sample with the same moisture content under the uniaxial compression. A possible reason is that the overall strength of coal samples with high moisture contents is partially low, and thus, the change laws of peak strength under different loading modes can be hardly distinguished.

According to the PRC National Standard (GB/T 25217.2-2010), the dynamic failure time D_T means the duration from peak strength to complete specimen failure in the uniaxial compression test. The impact energy index K_E refers to the accumulative deformation energy before the peak value leading to the sample failure, and the deformation energy consumed after the peak value is reached in the uniaxial compression test. The elastic energy, an index used to measure the burst tendency of coal-rock mass, is the ratio of the elastic energy to the plastic strain energy in the cyclic loading/unloading test: the greater the W_{ET} value, the smaller the energy dissipated in the specimen loading process, namely, the stronger the release of kinetic energy will be.

$$W_{ET} = \frac{U_2}{U_1}, \tag{6}$$

where U_1 is the plastic strain energy, being the area of the hysteretic loop in the ith cycle; and U_2 is the elastic strain energy, being the area under the ith unloading curve.

According to the PRC National Standard (GB/T 25217.2-2010), the coal samples in this test showed a weak burst tendency. The burst tendency of coal was divided into three types on the basis of the related indexes, as listed in Table 4. When four indexes were contradictory, the classification could be implemented using the fuzzy comprehensive evaluation method. With the increase in moisture content, the elastic energy index W_{ET} is reduced from 6.52256 (strong impact) to 2.69984 (weak impact), impact energy index K_E from 6.36 (strong impact) to 2.06 (weak impact), uniaxial compressive strength σ from 3.94 (weak impact) to 1.71 (no impact), and dynamic failure time D_T from 64.3 ms (weak impact) to 193.34 ms (weak impact). Fundamentally, the burst tendency of the coal sample is reduced after containing moisture. Higher moisture content contributed to more obvious reduction amplitude, further indicating that the coal sample with a high moisture content experiences a failure by absorbing less energy, thus mitigating its burst tendency. Given this, the feasibility and theoretical reasonability of coal seam water injection in the prevention and control of rock burst are verified through the test.

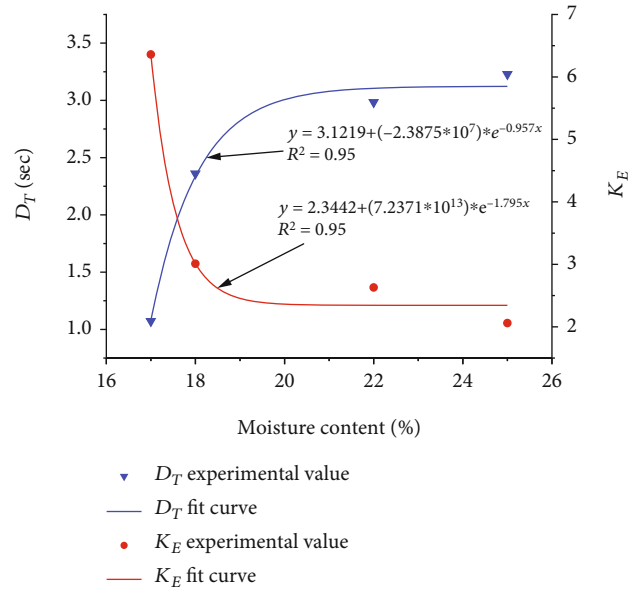

Figure 7: Fitted curves of dynamic failure time and impact energy index of coal samples with different moisture contents.

Figure 7 and Table 5 reveal that as the moisture content increases, the dynamic failure time is gradually lengthened, and they have a positive correlation, whereas the impact energy index is negatively correlated with the moisture content, possibly because the water molecules change the structure and connection type of particles inside the coal sample. Unloading cannot be timely realized in case of

Table 5: Test values of burst tendency of some coal samples.

Loading condition	No.	Moisture content	Dynamic failure time D_T (ms)	Impact energy index K_E	Elastic energy index W_{ET}
Uniaxial compression failure	a2	17%	64.3	6.36	—
	a4	18%	141.6	3.01	—
	a8	22%	179.1	2.63	—
	a9	25%	193.34	2.06	—
Cyclic loading/unloading	b3	18%	—	—	6.52256
	b6	21%	—	—	4.47789
	b9	25%	—	—	2.69984

failure of the coal sample with high moisture content, the potential energy accumulated inside it fails to be timely dissipated, and thus, long unloading time is needed. The peak stress inducing the sample failure and elasticity energy W_{ET} were gradually reduced with the increase in moisture content, indicating that the existence of water can reduce the elastic limit of the coal sample, soften the rock, and easily lead to deformation and failure of the coal sample. However, as the moisture content continuously increases, the weakening effect of water on coal strength is gradually alleviated, while the coal with a high moisture content would maintain a certain strength.

Based on the data acquired by the DS5 AE system, the AE energy count and ring-down count of some coal samples were selected in this study. Accumulative energy—energy of mathematical meaning—reflects the intensity of the relative energy of the AE signal, and it is calculated as the area under the detection envelop line of the AE signal; ring-down count reflects the number of AE events, and it has a certain corresponding relation with the internal damage degree of rock material [42, 43].

From the ring-down count and stress-strain curves as shown in Figure 8, the peak value of AE ring-down count appears nearby the peak stress. In the initial compaction phase, the early stage AE signal of the coal sample was obviously weak due to the softening and lubricating effects of water, and almost no AE signal is generated; in the elastic and yield phases, the AE signal of each sample is obviously enhanced; in case of coal failure, microcracks can be intuitively observed, accompanied by the sharp increase in AE ring-down count. The peak value of AE ring-down count lags behind the peak stress, and the ring-down count is still generated after the coal sample reaches the peak stress. However, under an excessively high moisture content, the lag time is shortened, indicating, again, that under an extremely high moisture content in the coal sample, the generation of AE events in the sample is weakened, namely, the ability of water molecules to change the internal structure of the coal sample is limited.

By analyzing the accumulative energy and stress-strain curves in Figure 8, each coal sample experiences a slow increase in energy in the initial phase, and the sharp increase in energy can be obviously observed before the coal failure. As natural soaking is adopted to treat the coal samples, the bonding ability between coal particles is degraded due to the action of moisture, and the energy needed by the coal sample to reach the peak stress is reduced. The accumulative energy in case of coal failure presents a gradual declining trend, demonstrating that the coal sample with a higher moisture content absorbs less energy when going through a failure. As shown in Figure 8(b), the accumulative energy is still increasing after the peak stress, because after the coal sample reaches the peak stress, the AE probe fails to be fixed around the sample. As the test proceeds, a slight collision takes place between the probe and the wall surface of the coal pillar. The curves in Figure 8(c) are not continuously changed with the implementation of this test, because the coal sample is already completely damaged during the loading process, the AE probe falls off, and thus the complete data cannot be acquired.

The moisture content has a bearing on the form of coal failure in addition to its strength. As shown in Figure 9, the failure modes of coal samples are analyzed. The coal samples mainly experience tensile fracture failure, and meanwhile, a small number of shear cracks are generated. By comparing the crack development in Figure 10, the red line represents macrocrack. With the increase in moisture content, the coal failure form gradually tends to be a tensile failure, and as for their morphological characteristics, they are run through by tensile cracks. These cracks are fully developed, and the fragment shedding phenomenon occurs to some coal samples in case of failure. The tensile cracks are not obvious in the coal sample with the moisture content of 16%, possibly because the coal sample experiences a failure under the insufficient development of the tensile fracture failure.

4. Conclusions

The mechanical properties, energy storage characteristics, and failure modes of moisture-containing coal samples are analyzed through the uniaxial compression test, loading/unloading test, and AE test. Ultimately, the following conclusions were drawn:

(1) As the moisture content increases, the duration of the elastic phase in the loading-induced coal failure is shortened, while the duration of the plastic zone in

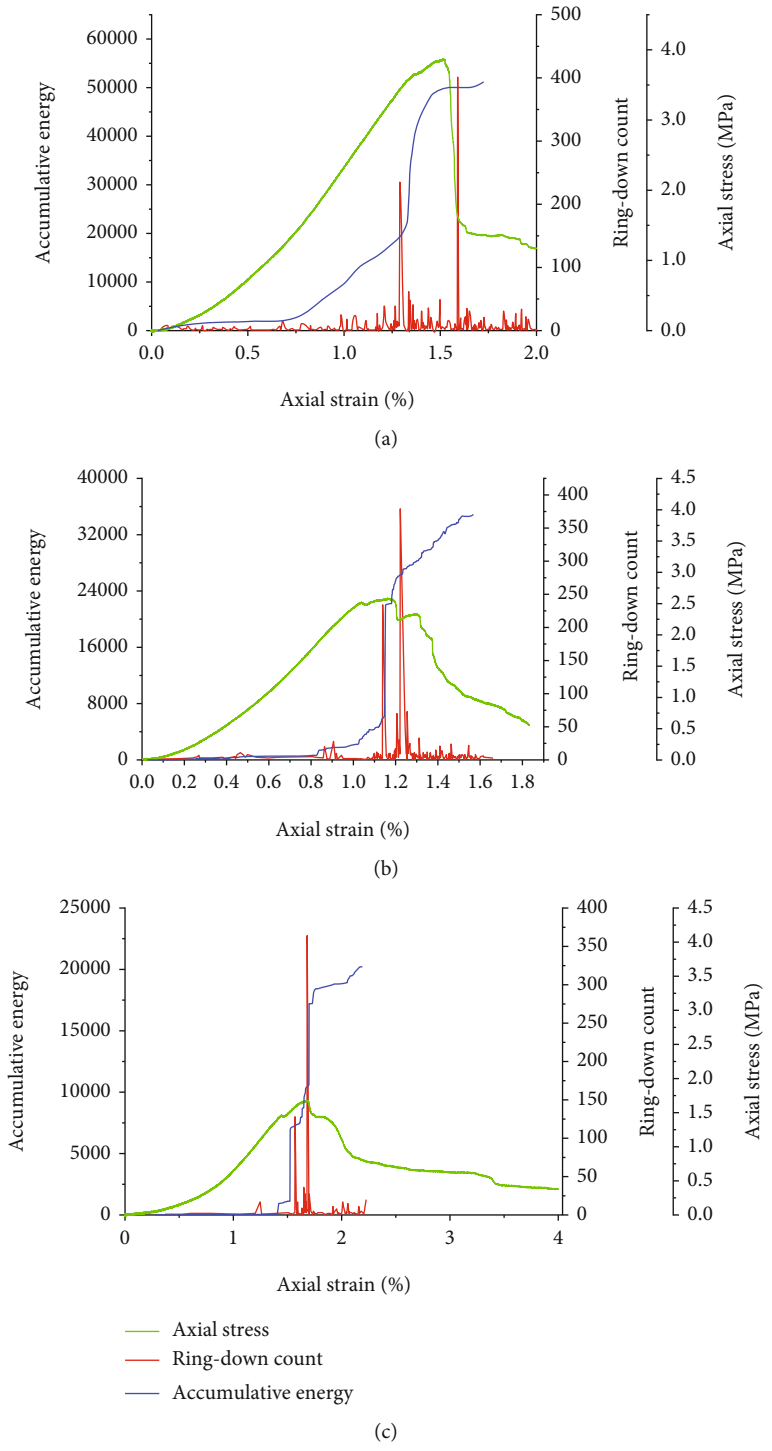

Figure 8: Stress-strain-accumulative energy-ring-down count curves under different moisture contents ((a) 17%; (b) 21%; (c) 25%).

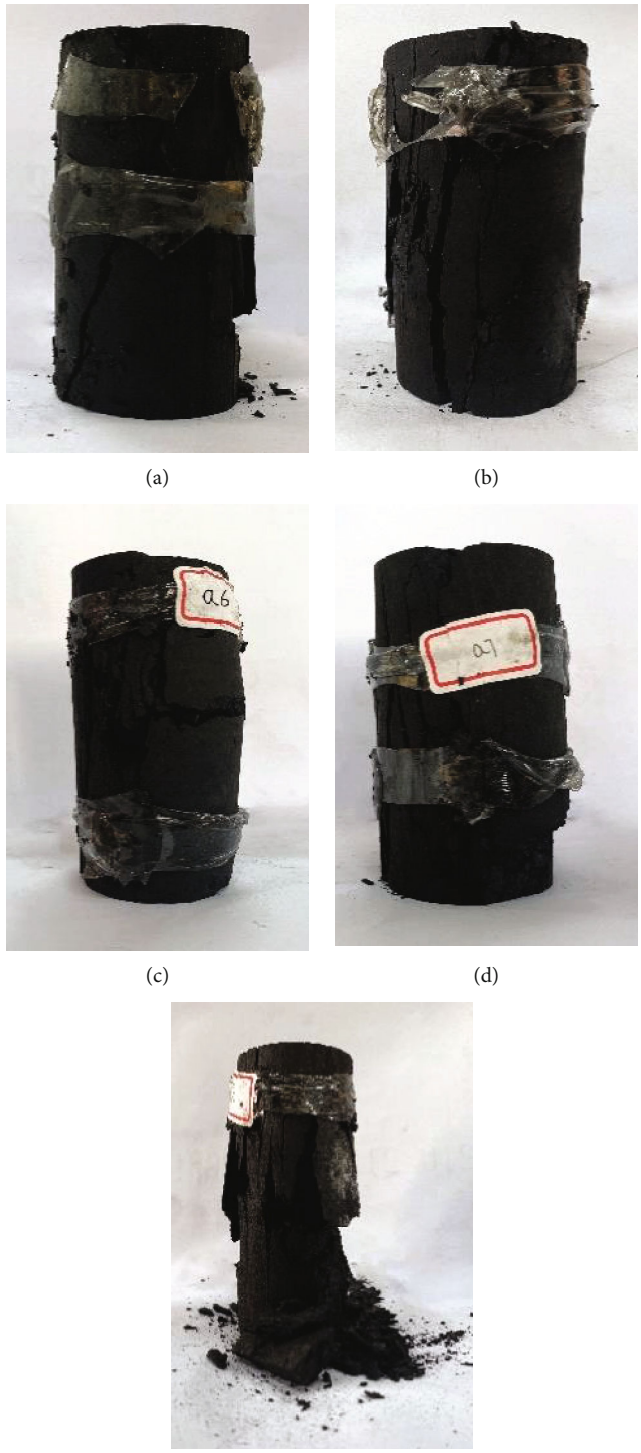

Figure 9: Broken states of coal samples with different moisture contents ((a) 16%; (b) 17%; (c) 20%; (d) 21%; (e) 25%).

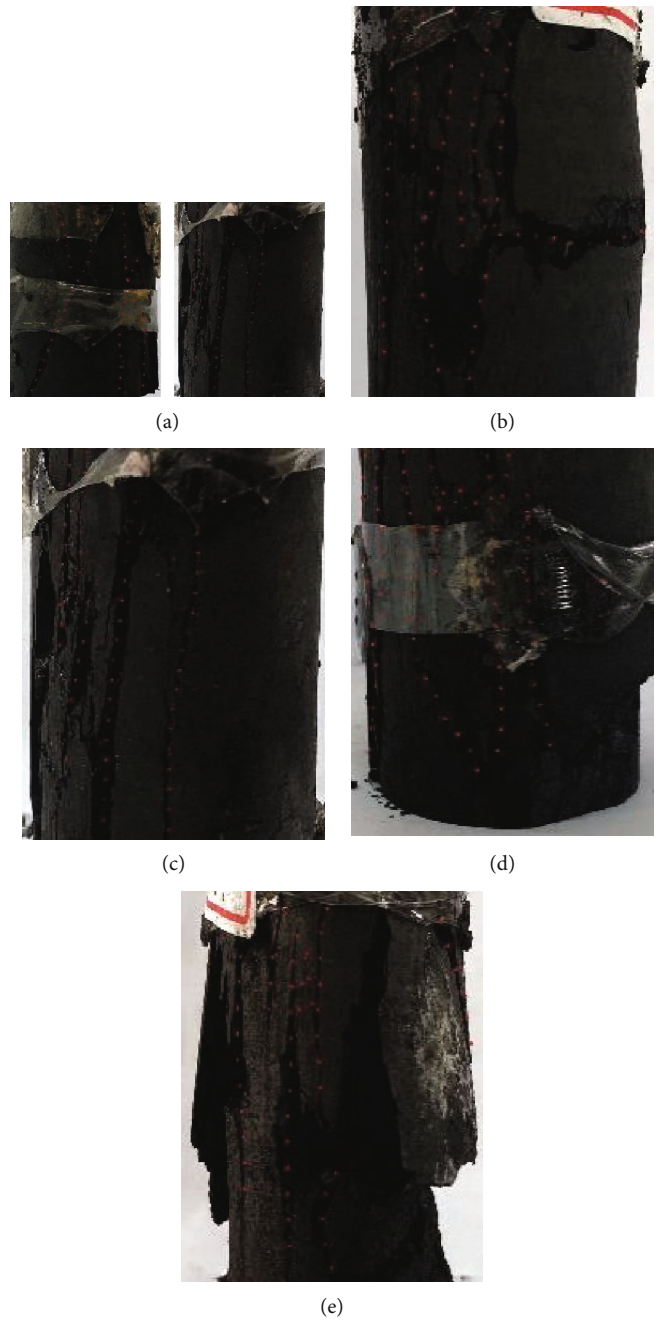

Figure 10: Local images of the broken states of coal samples with different moisture contents ((a) 16%; (b) 17%; (c) 20%; (d) 21%; (e) 25%).

the postpeak phase is lengthened. The higher moisture content leads to the lower peak strength and elastic modulus of coal, and the more obvious coal "softening"

(2) The peak stress leading to coal failure, area of the hysteretic loop, and elastic energy index W_{ET} decline with the increase in moisture content. The impact energy index K_E is negatively correlated with the moisture content, and the dynamic failure time D_T positively correlates with the moisture content, but as the moisture content continues to increase, this variation trend is gradually mitigated, indicating that when the coal sample goes through a failure after containing moisture, the accumulative elastic energy is reduced, so is the burst tendency. However, when the moisture content approaches the saturated state, the weakening effect of water on coal strength is gradually mitigated, and the coal sample with a high moisture content retains a certain strength

(3) The number of AE events shows an excellent corresponding relation with the complete stress-strain laws of coal samples. The coal failure is accompanied

by the sharp increase in AE ring-down count, which lags behind the peak stress, and is still generated after the coal sample reaches the peak stress. The tensile failure is a dominant failure mode of the coal sample, along with a small quantity of shear failure. With the increase in moisture content, the failure mode is gradually inclined to tensile failure, and the fragment shedding phenomenon occurs to some coal samples in case of failure

Data Availability

All data generated or analyzed during this study are included in this published article.

Conflicts of Interest

The authors declare no conflict of interest.

Authors' Contributions

Chuanming Li and Nan Liu designed the experiments; Nan Liu, Xin Xia, and Xiang Gao carried out the experiments; Nan Liu and Chuanming Li analyzed the experimental results; Nan Liu and Ruimin Feng wrote the manuscript.

Acknowledgments

This research was supported by the Anhui Provincial Natural Science Foundation (2008085ME147) and open foundation from the Key Laboratory of Coal Mine Safety and Efficiently Caving of Ministry of Education (JYBSYS2018102).

References

[1] H. Y. Li, Y. L. Mo, and Z. X. Sun, "Research status and prospect of coal bumps prevention and control technology," *Coal Science and Technology*, vol. 47, no. 1, pp. 62–68, 2019.

[2] Y. S. Pan and L. P. Dai, "Theoretical formula of rock burst in coal mines," *Journal of China Coal Society*, vol. 46, no. 3, pp. 789–799, 2021.

[3] D. X. Zhang, W. Y. Guo, C. W. Zang et al., "A new burst evaluation index of coal–rock combination specimen considering rebound and damage effects of rock," *Geomatics, Natural Hazards and Risk*, vol. 11, no. 1, pp. 984–999, 2020.

[4] H. C. Zhou, C. Z. Jia, and H. F. Jiang, "Influence of water injection on impact tendency of hard rock," *Inner Mongolia Coal Economy*, vol. 4, no. 10, pp. 127–147, 2018.

[5] B. Liang, M. Tian, and J. G. Wang, "Effect of different water contents on bursting potential of hard coal seam," *Journal of Water Resources & Water Engineering*, vol. 25, no. 1, pp. 100–102, 2014.

[6] C. X. Wan, "Effect of different moisture state on coal bursting tendency," *Opencast Mining Technology*, vol. 4, no. 2, pp. 31–35, 2015.

[7] C. B. Jiang, M. K. Duan, G. Z. Yin, G. P. Wu, and H. Yu, "Loading-unloading experiments of coal containing gas under the condition of different moisture contents," *Journal of China Coal Society*, vol. 41, no. 9, pp. 2230–2237, 2016.

[8] Z. L. Zhou, X. Cai, Y. Zhao, L. Chen, C. Xiong, and X. B. Li, "Strength characteristics of dry and saturated rock at different strain rates," *Transactions of Nonferrous Metals Society of China*, vol. 26, no. 7, pp. 1919–1925, 2016.

[9] H. R. Li, R. Shen, D. Li et al., "Acoustic emission multi-parameter analysis of dry and saturated sandstone with cracks under uniaxial compression," *Energies*, vol. 12, no. 10, p. 1959, 2019.

[10] Z. L. Zhou, X. Cai, W. Cao, X. Li, and C. Xiong, "Influence of water content on mechanical properties of rock in both saturation and drying processes," *Rock Mechanics and Rock Engineering*, vol. 49, no. 8, pp. 3009–3025, 2016.

[11] Z. A. Erguler and R. Ulusay, "Water-induced variations in mechanical properties of clay-bearing rocks," *International Journal of Rock Mechanics and Mining Sciences*, vol. 46, no. 2, pp. 355–370, 2009.

[12] C. M. Li, N. Liu, and W. R. Liu, "Experimental investigation of mechanical behavior of sandstone with different moisture contents using the acoustic emission technique," *Advances in Civil Engineering*, vol. 2020, Article ID 8877921, 10 pages, 2020.

[13] H. Karakul and R. Ulusay, "Empirical correlations for predicting strength properties of rocks from P-wave velocity under different degrees of saturation," *Rock Mechanics and Rock Engineering*, vol. 46, no. 5, pp. 981–999, 2013.

[14] C. Tang, Q. Yao, Z. Li, Y. Zhang, and M. Ju, "Experimental study of shear failure and crack propagation in water-bearing coal samples," *Energy Science & Engineering*, vol. 7, no. 5, pp. 2193–2204, 2019.

[15] Z. Li and D. J. Reddish, "The effect of groundwater recharge on broken rocks," *International Journal of Rock Mechanics and Mining Sciences*, vol. 41, pp. 280–285, 2004.

[16] J. D. Jiang and J. Xu, "Investigation of energy mechanism and acoustic emission characteristics of mudstone with different moisture contents," *Shock and Vibration*, vol. 2018, Article ID 2129639, 11 pages, 2018.

[17] D. Y. Li, L. N. Y. Wong, G. Liu, and X. Zhang, "Influence of water content and anisotropy on the strength and deformability of low porosity meta-sedimentary rocks under triaxial compression," *Engineering Geology*, vol. 126, pp. 46–66, 2012.

[18] X. T. Feng, Y. H. Gao, X. W. Zhang, Z. Wang, Y. Zhang, and Q. Han, "Evolution of the mechanical and strength parameters of hard rocks in the true triaxial cyclic loading and unloading tests," *International Journal of Rock Mechanics and Mining Sciences*, vol. 131, p. 104349, 2020.

[19] R. Qian, G. Feng, J. Guo, P. Wang, and H. Jiang, "Effects of water-soaking height on the deformation and failure of coal in uniaxial compression," *Applied Sciences*, vol. 9, no. 20, p. 4370, 2019.

[20] G. Cheng, C. Tang, L. Li, X. Chuai, T. Yang, and L. Wei, "Micro-fracture precursors of water flow channels induced by coal mining: a case study," *Mine Water and the Environment*, vol. 40, no. 2, pp. 398–414, 2021.

[21] Z. Chong, X. Li, J. Lu, T. Chen, J. Zhang, and X. Chen, "Numerical investigation of acoustic emission events of argillaceous sandstones under confining pressure," *Mathematical Problems in Engineering*, vol. 2017, Article ID 7676417, 16 pages, 2017.

[22] L. Yu, Q. Yao, X. Li, W. Wang, H. Han, and M. Zhang, "Experimental study of failure characteristics and fissure propagation in hydrous siltstone," *Arabian Journal of Geosciences*, vol. 13, no. 13, 2020.

[23] The Japanese Society for Non Destructive Inspection, *Practical Acoustic Emission Testing*, Springer, Tokyo, Japan, 2016.

[24] L. I. Tian-bin, C. H. Zi-quan, C. H. Guo-qing, M. Chun-chi, T. Ou-ling, and W. Min-jie, "An experimental study of energy mechanism of sandstone with different moisture contents," *Rock and Soil Mechanics*, vol. 36, no. S2, pp. 229–236, 2015.

[25] H. Q. Wu, F. Y. Ren, and D. Xia, "Damage deformation and acoustic emission characteristics of raw coal under different moisture contents," *Tehnički vjesnik*, vol. 27, no. 4, 2020.

[26] Y. A. O. Qiang-ling, L. I. Xue-hua, H. E. Li-hui, and Z. H. O. U. Jian, "Strength deterioration and acoustic emission characteristics of water-bearing sandstone in uniaxial compressive experiment," *Journal of Mining & Safety Engineering*, vol. 30, no. 5, pp. 717–722, 2013.

[27] C. J. Chen, Y. J. Zhao, S. L. Guo, L. Zhao, and Y. T. Pan, "Experimental study on acoustic emission characteristics of coal with different moisture content," *Safety in Coal Mines*, vol. 49, no. 5, 2018.

[28] X. D. Li, *Study on acoustic emission test and impact tendency in the failure process of coal rock sample, [M.S. thesis]*, China University of Mining and Technology, 2020.

[29] V. Rudajev, J. Vilhelm, and T. Lokajíček, "Laboratory studies of acoustic emission prior to uniaxial compressive rock failure," *International Journal of Rock Mechanics and Mining Sciences*, vol. 37, no. 4, 2000.

[30] P. Zhang, Z. P. Meng, K. Zhang, and S. Jiang, "Impact of coal ranks and confining pressures on coal strength, permeability, and acoustic emission," *International Journal of Geomechanics*, vol. 20, no. 8, article 04020135, 2020.

[31] X. Fu, Y.-X. Ban, Q. Xie, R. A. Abdullah, and J. Duan, "Time delay mechanism of the Kaiser effect in sandstone under uniaxial compressive stress conditions," *Rock Mechanics and Rock Engineering*, vol. 54, no. 3, pp. 1091–1108, 2021.

[32] Q. L. Yao, W. N. Wang, L. Zhu, Z. Xia, C. Tang, and X. Wang, "Effects of moisture conditions on mechanical properties and AE and IR characteristics in coal–rock combinations," *Arabian Journal of Geosciences*, vol. 13, no. 14, 2020.

[33] F. K. Xiao, "Analysis on warning signs of damage of coal samples with different water contents and relevant damage evolution based on acoustic emission and infrared characterization," *Infrared Physics and Technology*, vol. 97, pp. 287–299, 2019.

[34] R. S. Yang, Y. Li, D. Guo, L. Yao, T. Yang, and T. Li, "Failure mechanism and control technology of water-immersed roadway in high- stress and soft rock in a deep mine," *International Journal of Mining Science and Technology*, vol. 27, no. 2, pp. 245–252, 2017.

[35] T. Teng and P. Gong, "Experimental and theoretical study on the compression characteristics of dry/water-saturated sandstone under different deformation rates," *Arabian Journal of Geosciences*, vol. 13, no. 13, 2020.

[36] C. Z. Cen, Y. F. Jiang, and C. J. Jiang, "Experiment and analysis about the change of elasticity modulus of coal with different water contained," *Value Engineering*, vol. 34, no. 24, pp. 154-155, 2015.

[37] E. Eberhardt, D. Stead, B. Stimpson, and R. S. Read, "Identifying crack initiation and propagation thresholds in brittle rock," *NRC Research Press Ottawa, Canada*, vol. 35, no. 2, 1998.

[38] Z. P. Meng, J. N. Pan, L. L. Liu, G. X. Meng, and Z. H. Zhao, "Influence of moisture contents on mechanical properties of sedimentary rock and its bursting potential," *Chinese Journal of Rock Mechanics and Engineering*, vol. 28, no. S1, pp. 2637–2643, 2009.

[39] C. J. Wu, T. Qin, Z. W. Liu, and G. Liu, "Study on mechanical properties and energy evolution law of coal samples with different impact tendency," *China Mining Magazine*, vol. 30, no. 2, pp. 160–166, 2021.

[40] C. Li, N. Liu, W. Liu, and R. Feng, "Study on characteristics of energy storage and acoustic emission of rock under different moisture content," *Sustainability*, vol. 13, no. 3, p. 1041, 2021.

[41] W. Cai, L. Dou, G. Si, A. Cao, J. He, and S. Liu, "A principal component analysis/fuzzy comprehensive evaluation model for coal burst liability assessment," *International Journal of Rock Mechanics and Mining Sciences*, vol. 81, pp. 62–69, 2016.

[42] D. Xia, T. Yang, T. Xu, P. Wang, and Y. Zhao, "Experimental study on AE properties during the damage process of water-saturated rock specimens based on time effect," *Journal of China Coal Society*, vol. 40, no. S2, pp. 337–345, 2015.

[43] C. Grosse and M. Ohtsu, *Acoustic Emission Testing*, Springer, 2008.